Progress Towards Atmospheric Correction for Aerospace Electric Discharge Applications

Sofia P. Mavidou, David Clark and A. Manu Haddad

Cardiff University, Advanced High-Voltage Engineering Research Centre, The Parade, CF24 3AA, Cardiff, Wales, UK

{MavidouS, ClarkD, Haddad}@cardiff.ac.uk

Keywords: Partial Discharges, Electric Breakdown, Low Pressure, More-Electric Aircraft

1. ABSTRACT

In combating the threat of irreversible climate change, all sectors will need to reduce their carbon dioxide emissions and wider environmental impact. In addition, the rising cost of fuel and maintenance and the quest for continual improvement in aircraft performance has led the aviation industry to the challenge of transitioning from traditional mechanical systems and subsystems to electrical equivalents. In this work, different electrode configurations, simulating the divergent field distributions present in aircraft electrical systems, are examined with adjustable gap distance and variable pressure to simulate flying altitudes. The temperature and humidity in the test vessel are monitored continuously during the tests, but not controlled. We present initial results showing the effect of atmospheric pressure on the partial discharge inception and breakdown voltages in standard electrode configurations.

2. INTRODUCTION

In aircraft applications, electrical systems must operate under harsh environmental conditions and, in the more electric aircraft concept, at higher voltage levels. That combination becomes very challenging for the designers of electrical insulation systems due to the high risk of partial discharge occurrence around wires and other regions of high electric fields. Currently, the Paschen minimum for electrical discharges is the adopted maximum criterion for sizing and separation of wires on board [1]. The electric field around a high voltage conductor, a connection or termination of a wire or around any other component that is part of the electrical system is broadly the same at altitude as it is at ground level. The difference is the dielectric strength of the air which is pressure-dependent, so, insulation may need to be over-specified to compensate. Most fundamental empirical formulae and laws are well established for terrestrial electrical systems. Correction factors are applied to estimate the discharge thresholds at different conditions of temperature, pressure and humidity. In contrast, there is little published work concerning aeronautical atmospheric conditions and, hence, it is important to investigate the applicable correction factors for such highly variable conditions at flight altitudes [2].

In this study, we investigate the effect of pressure on the breakdown and partial discharge inception voltages of geometries for variable gap distance representing non-uniform electric fields. A simulated-altitude test chamber is used to replicate aeronautical atmospheric conditions of pressure, temperature and humidity [3]. The investigation is undertaken for short gaps because these are likely to be found in electrical systems within the aircraft. The case of air-solid dielectric system is also examined with the addition of a dielectric barrier on top of the ground electrode. It is observed from the obtained data, that the Paschen curve is not an ideal predictor for electrical discharges concerning non-uniform electric fields, with and without the presence of the solid dielectric, as expected. Employing data from Paschen's Law, Halleck has proposed a method [4] to predict partial discharges in air solid dielectric systems, and Maller and Srivastava have derived an expression [5] that also takes into account the electric field parameter. These methods were derived for atmospheric air. The work presented in this paper is an attempt to contribute to the work concerning low pressures.

Paschen's Law illustrates the dependence of the breakdown voltage on the pressure, p and the interelectrode gap, d. Data from the Paschen's Law plotted in the figures in the next sections are given by (1) [6]:

$$V_b = \frac{B \cdot (p \cdot d)}{\ln\left(\frac{A \cdot (p \cdot d)}{\ln(1/\gamma + 1)}\right)} \quad (1)$$

Where A and B are experimentally obtained coefficients and vary for different gases. In air, A=12 $Torr^{-1} \cdot cm^{-1}$ and B=365 $V \cdot cm^{-1}$ [6] are often used in the literature. The factor γ is electrode material dependent and its value is also calculated experimentally. In the literature, it is often taken as $\gamma=10^{-2}$. All values were converted to the units mentioned in the plots before being plotted.

From the literature and work in this paper, it is expected that the Paschen criterion won't be adequate for predicting the voltage levels at which partial discharges will be incepted, especially in regions with non-uniform field distributions. Therefore, in-depth research of the phenomena is needed to answer the questions raised for optimizing a system based on the More Electric Aircraft philosophy, without threatening the long-term reliability of the system.

3. EXPERIMENTAL SETUP

The test voltage waveform was generated by a National Instruments output module and amplified by a TREK Model 30/20A High Voltage Power Amplifier, with a gain of 3000 V/V. The amplified test voltage was applied to the electrode configuration positioned inside the controlled atmospheric test chamber, through a high voltage feedthrough and raised continuously until discharges were detected. The pressure was controlled by a dry scroll pump.

3.1 Breakdown Voltage Tests

Fig. 1 shows the experimental setup for breakdown voltage tests. The current was captured utilizing a current transformer having a ratio of 0.1 V/A. A current limiting resistor was connected in series with the high voltage side of the High Voltage Power Amplifier.

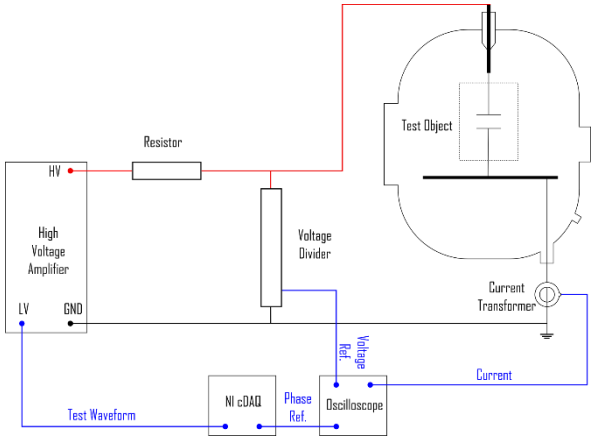

Fig.1. Experimental setup for breakdown voltage tests

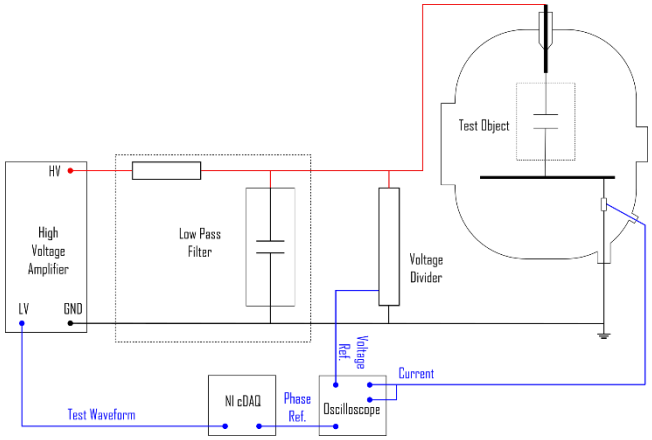

Fig. 2. Experimental setup for partial discharge tests

3.2 Partial Discharge Tests

Partial discharge tests were conducted in accordance with the general guidelines of IEC standard 60270 [7] and the experimental set up is shown in Fig. 2. Partial discharges were captured by a shunt resistance of 50 Ω.

3.3 Calibration of Measurement System

The calibration of the measurement system was carried out using a Haefely Tettex 9216 external calibrator. Fig. 3 and Fig. 4 show that the measured apparent charges of the captured pulses correspond to the known injected charges in the test circuit which ensures the accuracy of the measurement system.

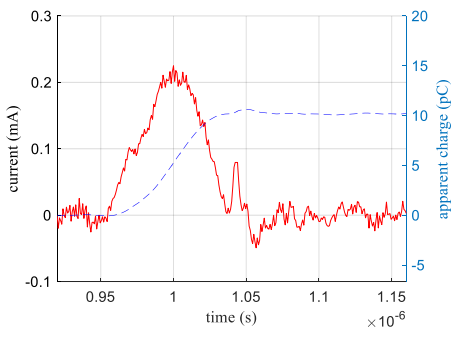

Fig. 3. Calibration pulse for charge injected value of 10 pC

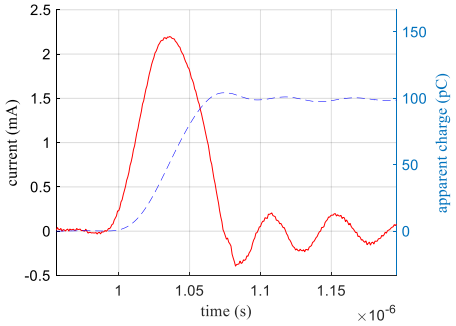

Fig. 4. Calibration pulse for charge injected value of 100 pC

4. TEST RESULTS

4.1 Rod – Plane Configuration

The pair of stainless-steel electrodes shown in Fig. 5 was placed inside the test chamber. The diameter of the plane ground electrode is 100 mm, and the diameter of the rod electrode is 5 mm. The tip of the rod is a hemisphere with radius 2.5 mm. Fig. 6 shows the computed maximum electric field norm and field efficiency factor for the rod – plane configuration for different gap length values. The field efficiency factor n was obtained from expression (2)[6]:

$$n = \frac{E_{mean}}{E_{max}} \tag{2}$$

where:

$$E_{mean} = \frac{V_{applied}}{g} \tag{3}$$

where g is the gap length and E_{max} was computed by finite element method simulation.

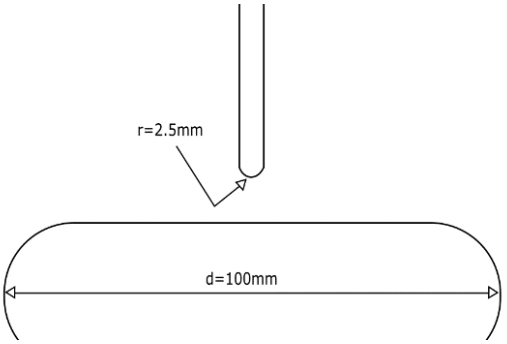

Fig. 5. Rod – plane configuration schematic

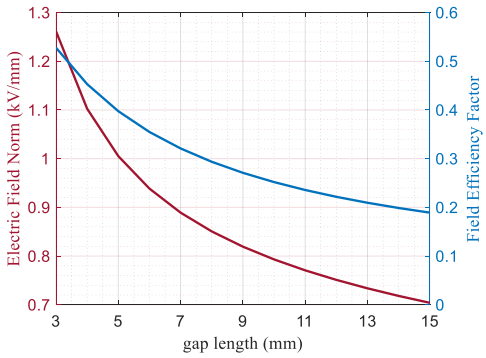

Fig. 6. Computed maximum electric field norm and field efficiency factor for rod – plane configuration for applied voltage; 2 kV

Tests were conducted to obtain the breakdown voltage values for gap distances d: 3, 6, 10 and 13 mm and pressures p: 1000, 800, 600, 400 and 200 mbar. Fig. 7 shows the breakdown voltage values obtained for product of pressures and gap distances cited above; 10 tests were performed per case and the standard deviation for each mean value is displayed in the plot. DC with negative and positive polarity was applied, raised continuously with a rate of rise of 2% of maximum test voltage per second, until breakdown of the air gap occurred.

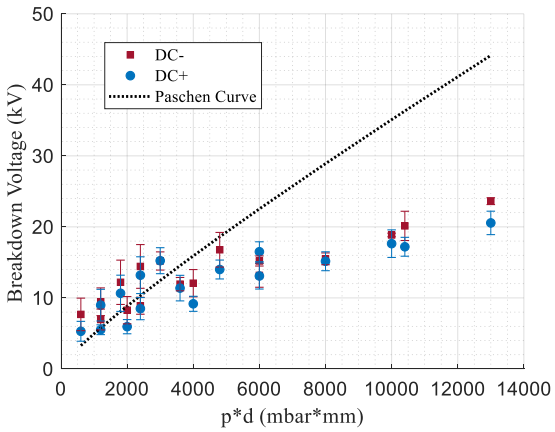

Fig. 7. Breakdown voltage values for gap distances; 3, 6, 10 and 13 mm and pressures; 1000, 800, 600, 400 and 200 mbar.

In the same figure, the Paschen curve is plotted for the range of the product of pressure and distance relevant to obtained results, to highlight the need for correction factors considering low pressure environments and non-uniform geometries. As expected from the literature, the lower the product of distance and pressure, the lower the breakdown voltage.

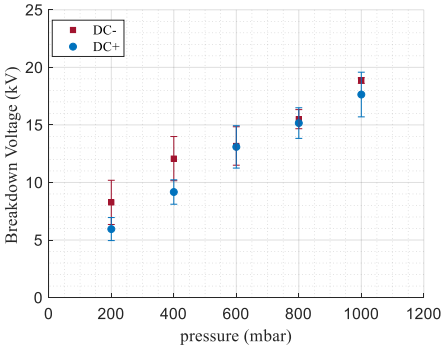

Fig. 8. Breakdown voltage values for gap distance; 10 mm and pressures; 1000, 800, 600, 400 and 200 mbar.

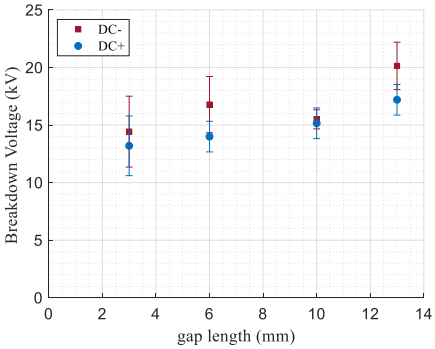

Fig. 9. Breakdown voltage values for gap distances; 3, 6, 10 and 13 mm and pressure; 800 mbar.

The breakdown voltage decreases with decreasing pressure for a fixed gap and increases with increasing gap for a constant pressure as shown in Fig. 8 and Fig. 9. It is observed that PDIV values have greater sensitivity to pressure.

Many experimental attempts were made to obtain values for Partial Discharge Inception Voltage (PDIV) for this configuration, but no partial discharge pulses could be observed prior breakdown of the interelectrode gap.

4.2 Rod – Plane Configuration with Dielectric Barrier

A 2 mm Polytetrafluorethylene (PTFE) barrier with 50 mm diameter as shown in Fig. 10, was introduced because of the proximity of the PDIV to the breakdown voltage and subjected to a similar test regime. Partial discharge pulses could not be observed with the addition of a PTFE barrier, either. Further attempts were made with long exposure imaging using a Nikon D7200 camera to investigate visually the presence of corona. Fig. 11 (a) and (b) show partial and full arcing of the interelectrode gap with no partial discharge activity captured prior to breakdown.

Fig. 10. Bright field image of rod – plane configuration with PTFE barrier

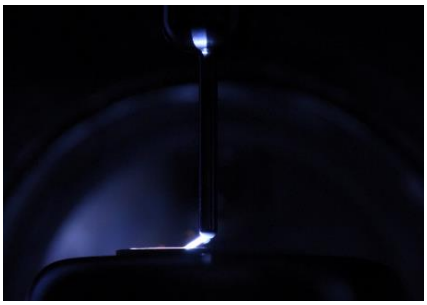

(a)

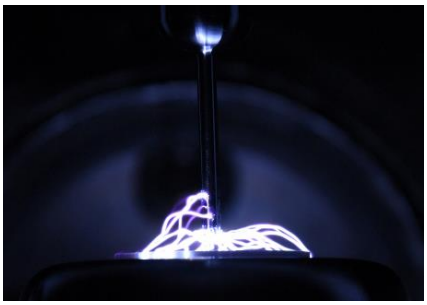

(b)

Fig. 11. Long exposure images of rod – plane configuration with PTFE barrier at 6 mm gap distance for pressures; (a) 400 mbar (b) 200 mbar. [DSLR camera settings: ISO:2000, f/5.6, Exposure: 30 s]

4.3 Needle – Plane Configuration with Dielectric Barrier

For the needle – plane configuration with a PTFE barrier shown in Fig. 12, tests were conducted for gap distances 5 and 6 mm resulting in air gap lengths d: 3 and 4 mm for pressures p: 1000, 800, 600, 400, 200 mbar and p: 900, 700, 500, 200, 100 mbar respectively. Fig. 13 shows the computed maximum electric field norm and field efficiency factor for the needle – plane configuration with PTFE barrier for different total gap length values.

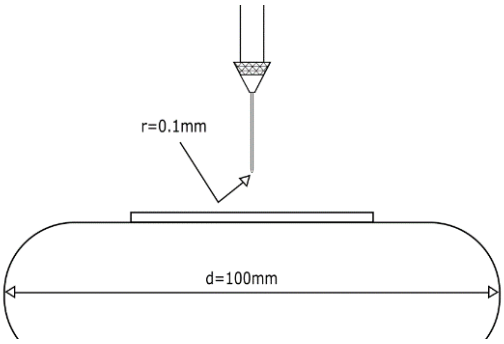

Fig. 12. Needle – plane configuration with PTFE barrier schematic

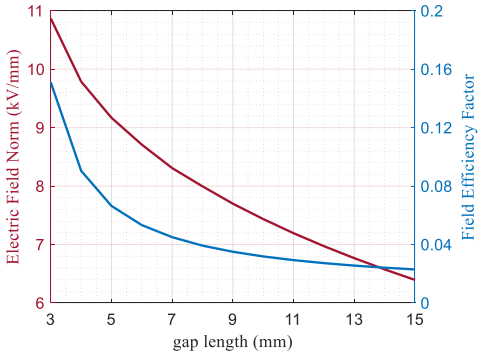

Fig. 13. Computed maximum electric field norm and field efficiency factor for needle – plane configuration with PTFE barrier for applied voltage; 2 kV

The radius of curvature of the tungsten needle electrode tip is 100 μm, and the diameter of the stainless-steel plane electrode is 100 mm.

Initially, tests were conducted at atmospheric air and AC voltage was applied. The configuration was tested with and without the PTFE barrier for three different total gap lengths and results are shown in Fig. 14. It is observed that the addition of the dielectric barrier at a fixed gap did not have an impact on the PDIV value. The needle – plane configuration with the dielectric barrier was chosen for the tests that were conducted at low pressures. One of the objectives of future work is to complete the dataset for the needle – plane configuration without the dielectric barrier.

Fig. 15 shows results referring to the air gap in order to make a comparison with the Paschen curve which is derived for air. Two different voltage waveforms were applied; AC and DC with negative polarity. The voltage was raised continuously with a rate of rise of 2% of maximum test voltage per second, until partial discharges were observed. For this configuration, 5 tests were done per case and the standard deviation for each mean value is displayed in the plot. As expected from the literature [8], for a given air gap, decreasing pressure resulted in decreasing PDIV values.

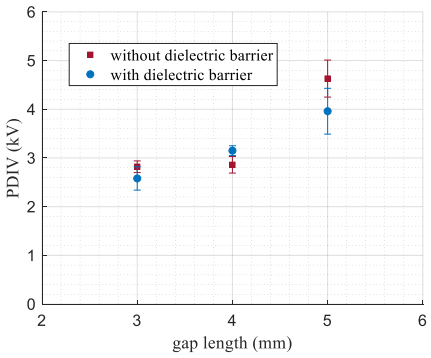

Fig. 14. PDIV values for AC at atmospheric pressure and total gap distances; 3, 4 and 5mm. Thickness of PTFE barrier; 2 mm.

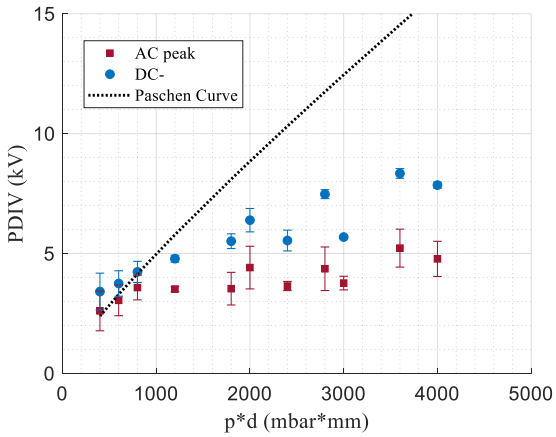

Fig. 15. PDIV values for air gap distances; 3, 4 mm and pressures; 1000, 800, 600, 400, 200 mbar and 900, 700, 500, 200, 100 mbar respectively.

Long exposure images were also captured for the needle – plane configuration with the PTFE barrier shown in the bright field image in Fig 16. Fig. 17 shows the partial discharge activity captured for the same exposure time at partial discharge inception levels for 1000, 600 and 200 mbar.

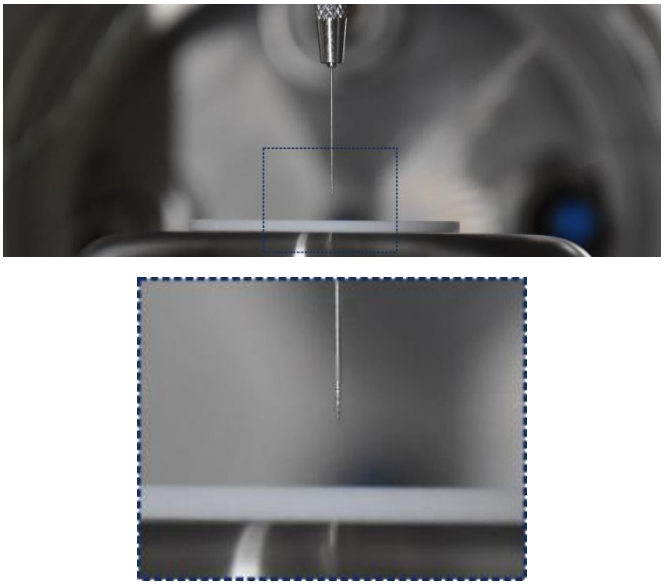

Fig. 16. Bright field image of needle – plane configuration with PTFE barrier

More partial discharge pulses were captured for the same exposure time for lower pressure levels which results in a brighter field around the tip of the needle. This indicates higher energy levels [9] and hence, could be more damaging for the insulation system and threaten its reliability.

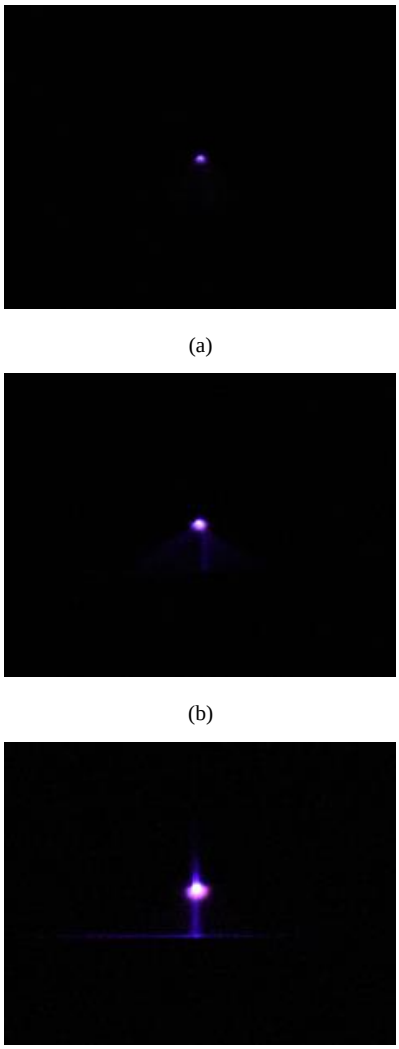

(a)

(b)

(c)

Fig. 17. Long exposure images of needle – plane configuration with PTFE barrier captured at partial discharge inception levels for pressures; (a) 1000 mbar, (b) 600 mbar and (c) 200 mbar [DSLR camera settings: ISO:2000, f/5.6, Exposure: 30 s]

5. CONCLUSIONS

In this paper, tests with two different electrode configurations were carried out at sub-atmospheric pressures and various gap distances in order to investigate the effect of pressure on the breakdown and partial discharge inception voltage for non-uniform field geometries. This is a precursor to work on more practical conductor and insulation geometries, and provides a useful fundamental grounding for that work. Results show that for a given air gap, partial discharge inception and breakdown voltage values decrease with decreasing pressure, as expected from the literature. Obtained values seem to follow the Paschen curve for smaller values of the product of pressure and distance but require a scaling factor as either pressure or gap distance increases. The scaling required, is likely to be a function of field efficiency factors and electrode spacing, and values are expected to differ for AC and DC.

Construction flaws during installation can result in non-uniform electric field regions around a wire connector or termination which combined with the harsh environmental conditions results in higher probability of Partial Discharges to occur. Therefore, it is critical that all cases of divergent electric fields are assessed before fully transitioning to electric aircrafts and higher operating voltages.

6. REFERENCES

[1] L. Lusuardi and A. Cavallini, "The Problem of Altitude When Qualifying the Insulating System of Actuators for More Electrical Aircraft," in 2018 IEEE International Conference on Electrical Systems for Aircraft, Railway, Ship Propulsion and Road Vehicles and International Transportation Electrification Conference, ESARS-ITEC, 2018, pp. 1–4. doi: 10.1109/ESARS-ITEC.2018.8607370.

[2] J. Rickmann, D. Tabakovic, C. Nyamupangedengu, N. Parus, D. Wu, and R. Diaz, "Atmospheric and altitude correction methods for air gaps and clean insulators - corrections for short gaps under DC and application difficulties - part 1," 2017.

[3] A. C. Mermigkas, D. Clark, and A. Manu Haddad, "Investigation of High Altitude/Tropospheric Correction Factors for Electric Aircraft Applications," in Lecture Notes in Electrical Engineering, 2020, vol. 598 LNEE, pp. 308–315. doi: 10.1007/978-3-030-31676-1_30.

[4] M. C. Halleck, "Calculation of Corona-Starting Voltage in Air-Solid Dielectric Systems," Transactions of the American Institute of Electrical Engineers. Part III: Power Apparatus and Systems, vol. 75, no. 3, pp. 211–216, 1956, doi: 10.1109/AIEEPAS.1956.4499294.

[5] V. N. Maller and K. D. Srivastana, "Corona inception phenomena in solid-air composite systems," IEEE Transactions on Electrical Insulation, vol. EI-18, no. 4, pp. 402–408, 1983, doi: 10.1109/TEI.1983.298679.

[6] J. Kuffel, W. S. Zaengl, and P. Kuffel, High Voltage Engineering Fundamentals. New York: Elsevier, 2000. doi: 10.1201/9781482290035.

[7] IEC 60270:2001, "High-voltage test techniques - Partial discharge measurements," 2001.

[8] D. Grosjean, D. Schweickart, D. Kasten, X. Liu, and S. Sebo, "The significance of partial discharge measurements for verification of insulation integrity in a low pressure environment," in Conference Record of the Twenty-Sixth International Power Modulator Symposium and High-Voltage Workshop, 2004, pp. 34–37. doi: 10.1109/modsym.2004.1433500.

[9] J. R. Riba, Á. Gómez-Pau, and M. Moreno-Eguilaz, "Insulation failure quantification based on the energy of digital images using low-cost imaging sensors," Sensors (Switzerland), vol. 20, no. 24, p. 7219, 2020, doi: 10.3390/s20247219.